JOURNAL OF MATERIALS SCIENCE 26 (1991) 1000–1008

Grain boundary sliding behaviour of copper and alpha brass at intermediate temperatures

S. V. RAJ
NASA Lewis Research Center, MS 49–1, 21000 Brookpark Road, Cleveland, Ohio 44135, USA

The role of grain boundary sliding in copper and Cu–30% Zn in the temperature range 0.50 to 0.72 T_m, where T_m is the absolute melting point of the material, is examined. First, sliding data obtained on these materials are presented. These results indicate that the stress exponent for sliding, n_{gbs}, is similar to that for lattice deformation, while the activation energy for sliding, Q_{gbs}, varies between about 0·5 Q_c and 1.6 Q_c, where Q_c is the activation energy for creep. Next, a comparison of the published values of Q_{gbs} for bicrystals and polycrystals suggests that grain boundary sliding in polycrystalline materials requires the accommodation of the sliding process, whereas in bicrystals, the absence of triple points and other grain boundaries results in intrinsic sliding. Finally, several models proposed for grain boundary sliding are discussed, and it is shown that they do not account for the observed results on copper and alpha brass. A phenomenological model is proposed, where it is assumed that grain boundary sliding results from the glide of dislocations on secondary slip planes.

1. Introduction

The current interest in developing materials for elevated temperature applications requires an understanding of the mechanisms controlling the creep behaviour of an engineering component during its lifetime. Typically, the range of temperatures in which these applications fall correspond to the intermediate temperature range between 0.3 and 0.7 T_m [1], where T_m is the absolute melting point of the material. At temperatures above 0.3 T_m, grain boundaries in a polycrystalline material attain an additional degree of freedom through the ability of neighbouring grains to slide past each other, and the amount of grain boundary sliding increases with temperature [2, 3]. In addition, the contribution of sliding to the total strain increases significantly for many materials as the stress [4–10] and grain size [3, 7, 8, 11, 12] decrease. Grain boundary sliding can influence the creep life of an engineering component significantly because it can lead to the nucleation of intergranular cracks and cavities, as well as to their possible growth and interlinkage. Therefore, a characterization of the sliding process, and an evaluation of the possible mechanisms governing this behaviour, can be useful in designing materials for elevated temperature applications.

At low and intermediate stresses, the steady-state strain rate, $\dot{\varepsilon}$, for lattice and boundary mechanisms can be usually represented by

$$\dot{\varepsilon} = A(D_0 G\boldsymbol{b}/kT)(\boldsymbol{b}/d)^p(\sigma/G)^n \exp(-Q_c/RT) \quad (1)$$

where D_0 is a frequency factor, G is the shear modulus, $\boldsymbol{b}$ the Burgers vector, k the Boltzmann constant, T the absolute temperature, d the grain size, σ the applied stress, Q_c the activation energy for the deformation mechanism, R the universal gas constant, and A, n and p are dimensionless constants. By definition, it follows that $p = 0$ for lattice mechanisms and $p \neq 0$ for boundary processes.

Grain boundary sliding mechanisms are classified into two broad categories: Lifshitz sliding and Rachinger sliding [13]. In the former process, the compatibility between the sliding grains is maintained by diffusional accommodation [14] either by Nabarro–Herring [15, 16] or Coble creep [17]. The main characteristic of Lifshitz sliding is that there is no change in grain neighbours. In contrast, Rachinger sliding, which is accommodated by plastic deformation inside the grains, results in a change in grain neighbours [18]. In general, grain boundary sliding at intermediate temperatures involves Rachinger sliding when dislocation creep is the dominant deformation mechanism in the grain interior.

The nature of the grain boundary sliding mechanisms in copper and alpha brass at intermediate temperatures is examined. The paper is divided into three parts: First, a review of recent experimental data obtained on copper and Cu–30% Zn [19] is presented and compared with those reported in other investigations. Second, it is demonstrated that none of the models proposed for grain boundary sliding are applicable to these observations. Third, a phenomenological model is postulated for grain boundary sliding behaviour in the intermediate temperature range.

2. Characteristics of grain boundary sliding in copper and alpha brass

Several techniques exist for measuring the displacement at a grain boundary due to sliding in a polycrystalline material, and these are reviewed elsewhere

0022–2461/91 $03.00 + .12

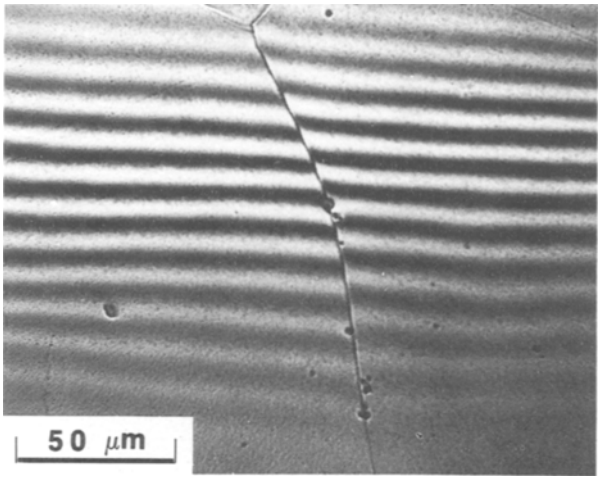

Figure 1 Interference fringes at a grain boundary in a polycrystalline copper specimen deformed to 3.1% at 873 K under a stress of 10.0 MPa illustrating the two-beam interferometry technique for measuring v_1: d = 250 μm.

[8]. A commonly used procedure is the two-beam interferometry technique where the vertical offset, v_1, at any position along a boundary can be determined from measurements of the fringe displacement. The technique is illustrated in Fig. 1, where it is seen that the fringes are displaced by about half a fringe width due to grain boundary sliding. The vertical offset is then given by

$$v_1 = N_0(\lambda/2) \quad (2)$$

where N_0 is the number of fringe displacements and λ is the wavelength of light ($\lambda/2$ = 0.3 μm in the present measurements). The error associated with an average value, $\bar{v}_1$, obtained from sliding measurements taken on 300 to 400 grain boundaries is typically about 10% [19]. The strain due to grain boundary sliding can be calculated from [8, 20]

$$\varepsilon_{gbs} = \varphi(\bar{v}_1/d) \quad (3)$$

where φ is a geometrical constant close to unity for many materials [8].

2.1 Displacement–time curves

Fig. 2 shows typical variations of ε and $\bar{v}_1$ with time, t, for selected polycrystalline copper specimens tested in the stress range 10.0 to 39.8 MPa and at temperatures between 673 and 900 K, respectively. The creep curves show a normal primary region after an instantaneous increase in strain followed by the secondary and tertiary creep regimes (Fig. 2a). The corresponding plots of $\bar{v}_1$ against t shown in Fig. 2b also exhibit a primary region of decreasing sliding rate after an initial grain boundary displacement, where the latter increases with stress and temperature. However, steady-state behaviour, consisting of a linear increase in $\bar{v}_1$ with t, is not observed in the grain boundary sliding curves shown in Fig. 2b, and this observation is fairly representative of variations of $\bar{v}_1$ with time at other stresses and temperatures. Instead, the grain boundary sliding rate tends towards zero as creep progresses as is evident for the data obtained at 873 K and 10.0 MPa. (It is important to note that due to experimental difficulties, only a limited number of data points could be obtained on each specimen in this investigation [19]. Two factors limited the number of measurements that could be made: an increase in the number of cracked and cavitated boundaries with creep strain, and a progressive tarnishing of the initially polished surface at longer times despite the fact that the specimens were tested in an argon atmosphere. Despite best efforts to measure the fringe displacements at as many boundaries as possible, it is possible that both these factors may have biased the measurements at the longer times and higher strains.) This decrease in the rate of sliding with time resulting from slide hardening has been observed in copper bicrystals [21] and other materials [22, 23].

Similar grain boundary sliding curves are observed for Cu–30% Zn, and Fig. 3 represents typical variations of ε and $\bar{v}_1$ with t for this alloy. The nature of the primary creep curve for this material was dependent on stress and temperature, and normal, sigmoidal, linear and inverse primary transients were observed

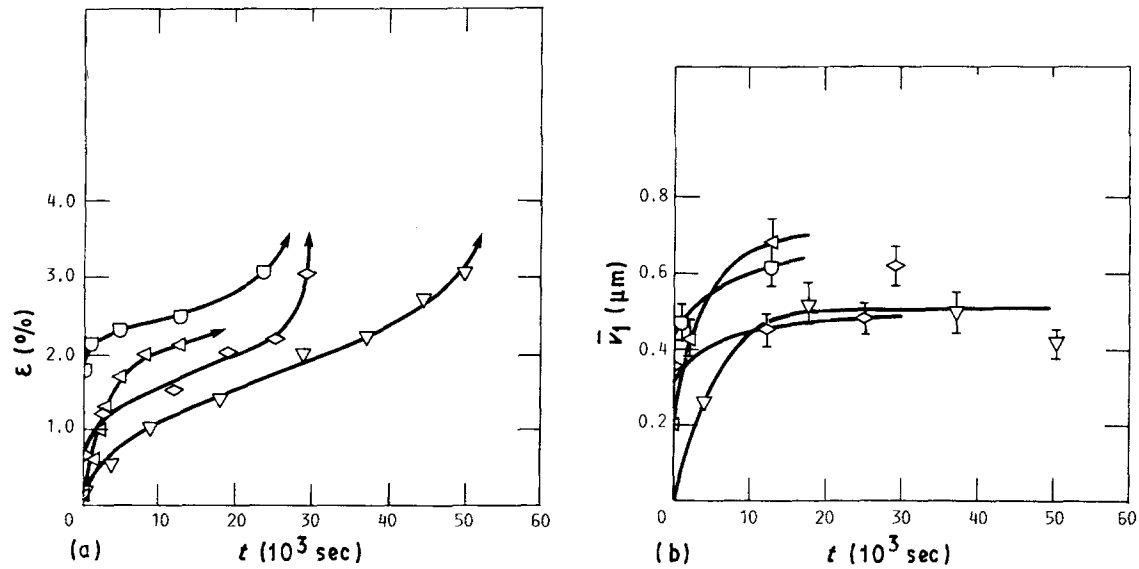

Figure 2 Plots of (a) ε–t and (b) $\bar{v}_1$–t curves for copper. d = 250 μm, (□) 673 K, 39.8 MPa; (◇) 773 K, 25.0 MPa; (▽) 873 K, 10 MPa; (◁) 898 K, 10 MPa.

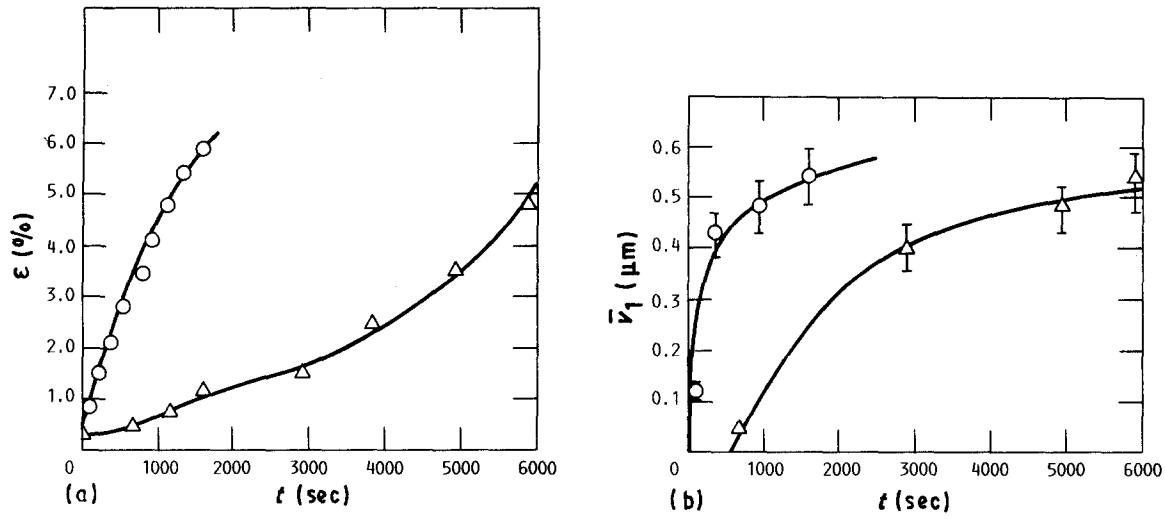

Figure 3 Plots of (a) ε–t and (b) $\bar{v}_1$–t curves for Cu–30% Zn. d = 120 μm, (△) 723 K, 39.9 MPa; (○) 773 K, 39.6 MPa.

under different conditions [19]. For example, sigmoidal and normal creep behaviour were observed at 723 and 773 K, respectively, under a stress of about 40 MPa (Fig. 3a). In general, there was an apparent correlation between the nature of the primary creep curve and the initial sliding behaviour. This is demonstrated in Fig. 3, where the $\bar{v}_1$–t plot at 723 K (Fig. 3b) exhibits an incubation period corresponding to the initial portion of the sigmoidal primary creep curve shown in Fig. 3a. Similarly, incubation periods were observed under stress and temperature conditions leading to inverse primary creep. However, normal primary creep did not result in an incubation period in the sliding curves (Fig. 3).

2.2. Effect of total strain

The above observations of slide hardening in copper and incubation periods in alpha brass suggest an apparent correlation between grain boundary sliding and intragranular deformation. This is demonstrated in Fig. 4 where ξ, defined as the ratio $\varepsilon_{gbs}/\varepsilon$, is plotted against the total strain, ε, for different stresses and temperatures. It is evident from Fig. 4 that grain-boundary sliding contributes significantly to the total strain within the first 0.5% of deformation in both materials. In copper this contribution is about 40% (Fig. 4a) while it is about 45% in alpha brass after an initial incubation strain of about 0.3% (Fig. 4b). However, ξ decreases sharply with increasing strain for $\varepsilon > 0.5\%$ so that the contribution from grain boundary sliding is less than 10% when $\varepsilon > 4\%$. The somewhat higher contribution from grain boundary sliding observed in the alloy can be attributed to its smaller grain size. As shown in Fig. 4, ξ is not significantly dependent on stress and temperature.

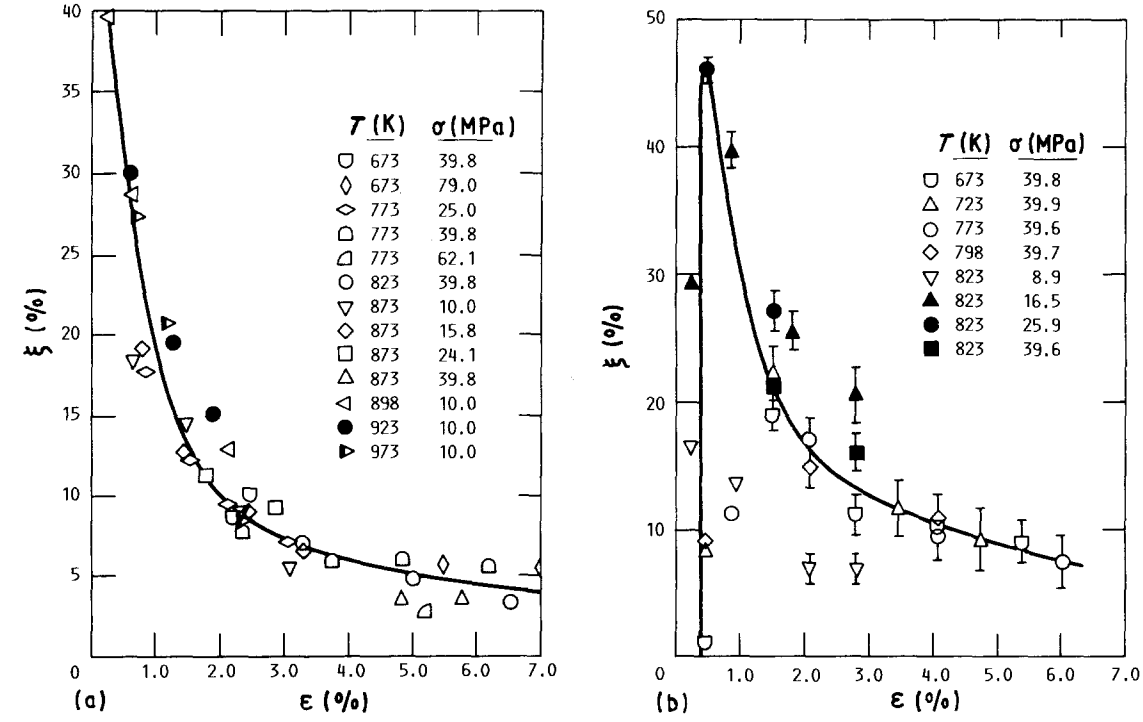

Figure 4 Variation of ξ with ε for (a) copper, d = 250 μm and (b) Cu–30% Zn, d = 120 μm.

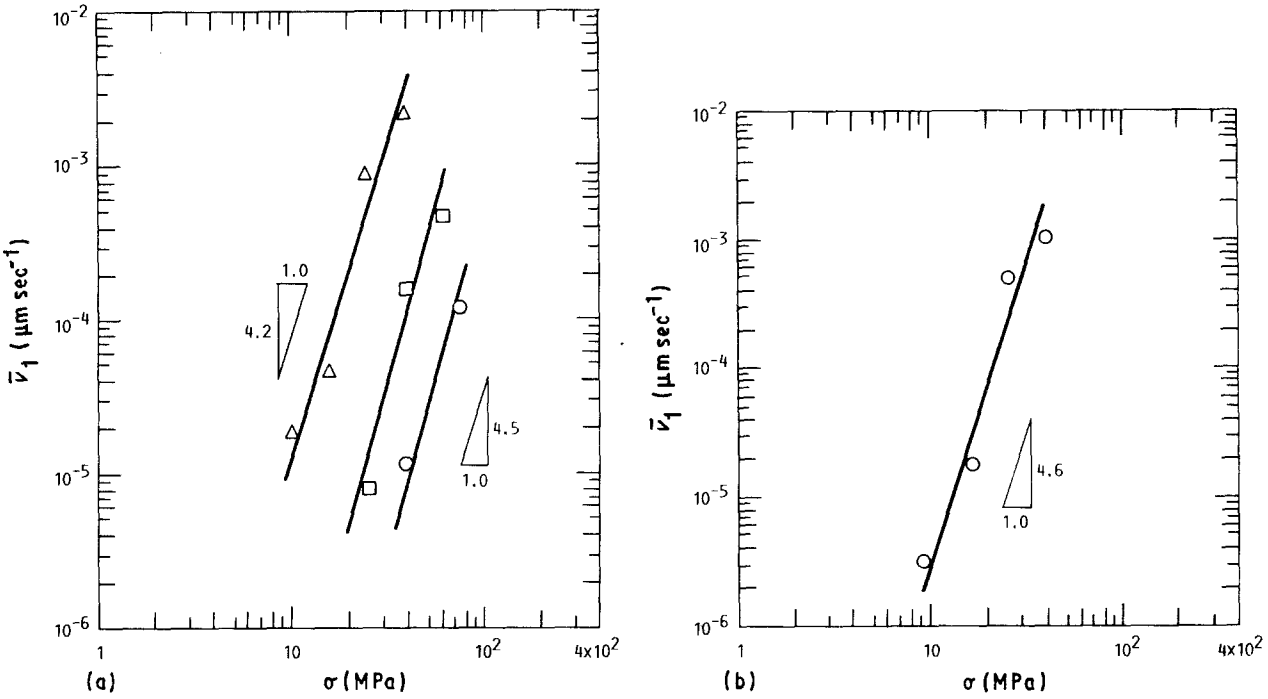

Figure 5 Stress dependence of $\dot{\bar{v}}_1$ for (a) copper, $d = 250$ μm and (b) Cu–30% Zn, $d = 120$ μm. T(K): (a) (○) 673, (□) 773, (△) 873; (b) 823.

2.3. Stress dependence of grain boundary sliding

Fig. 5 shows the stress dependence of the initial grain boundary sliding rate, $\dot{\bar{v}}_1$, where $\dot{\bar{v}}_1$ was evaluated from slopes of the increasing portion of the $\bar{v}_1$–t plots. The choice of the initial, rather than the steady-state sliding rates was influenced by the observed slide-hardening tendency in copper which made it impossible to evaluate the steady-state sliding rates in a consistent manner. The magnitude of the stress exponent for sliding, n_{gbs}, varies between 4.2 and 4.6 for both materials (Figs 5a and b). These values compare favourably with $n \approx 4.2$ for steady-state creep for these materials as shown in Fig. 6, where the initial sliding strain rate, $\dot{\varepsilon}_{gbs}$ (i.e. $\dot{\bar{v}}_1/d$) and $\dot{\varepsilon}$ are plotted against σ double logarithmically. The steady-state creep rate data on copper and Cu–30% Zn are reported elsewhere [19, 24]. Once again, these results are consistent with the idea that grain boundary sliding in these materials is influenced by lattice deformation. It is also evident from Fig. 6, that the initial sliding rates are significantly lower than the steady-state creep rates.

This similarity in the values of n and n_{gbs} is significant in view of the fact that it is not clear at present whether $n_{gbs} < n$ [25] or $n_{gbs} \approx n$ [26]. Langdon and Vastava [25] concluded from an examination of published data that generally $n_{gbs} < n$. However, Gifkins [26] has pointed out that such direct comparisons between data obtained from different investigations are probably invalid, partly because the experimental technique used for measuring grain boundary sliding varied from one investigation to another, and partly because the values of the stress exponents for creep were not always determined in the same study. Instead, he concluded from a re-analysis of the data reported in the original investigations, that $n_{gbs} \approx n$ in most instances. The results shown in Figs 5 and 6 are, therefore, consistent with the latter conclusions.

2.4. Temperature dependence of grain boundary sliding

Fig. 7 shows the variation of the temperature-compensated initial sliding rate against the inverse of the absolute temperature for these materials. As shown in Fig. 7a, the activation energy for sliding, Q_{gbs}, increases from about 120 kJ mol^{-1} at 39.8 MPa to about 280 kJ mol^{-1} at 10.0 MPa for copper. Similar values of Q_{gbs} are also obtained for Cu–30% Zn at a value of $\sigma = 39.7$ MPa (Fig. 7b), where $Q_{gbs} \approx 95$ kJ mol^{-1} for $T < 770$ K and $Q_{gbs} \approx 280$ kJ mol^{-1} when $T > 770$ K. In fact, if the stress dependence of $\dot{\bar{v}}_1$ is incorporated into the normalization parameters* as shown in Fig. 8, it becomes evident that these low and high values of activation energies may correspond to two independent deformation regimes. Alternatively, it is also possible to interpret these results as indicative of the dominance of a single mechanism with a range of stress and temperature-dependent values for Q_{gbs} varying between 100 and 325 kJ mol^{-1}, so that the data shown in Fig. 8 may be better represented by a smooth curve. These appear to be the first reported observations of a change in the magnitude of Q_{gbs} with temperature (and stress) for polycrystalline materials.

The activation energy for creep of copper was found to be stress dependent varying between about 180 kJ mol^{-1} at $\sigma/G = 3 \times 10^{-4}$ and about

* Note that the data tend to come together when a value of $n_{gbs} = 4.2$ is used in the normalizing parameter. This confirms that the magnitude of $n_{gbs} \approx n \approx 4.2$ determined earlier is correct.

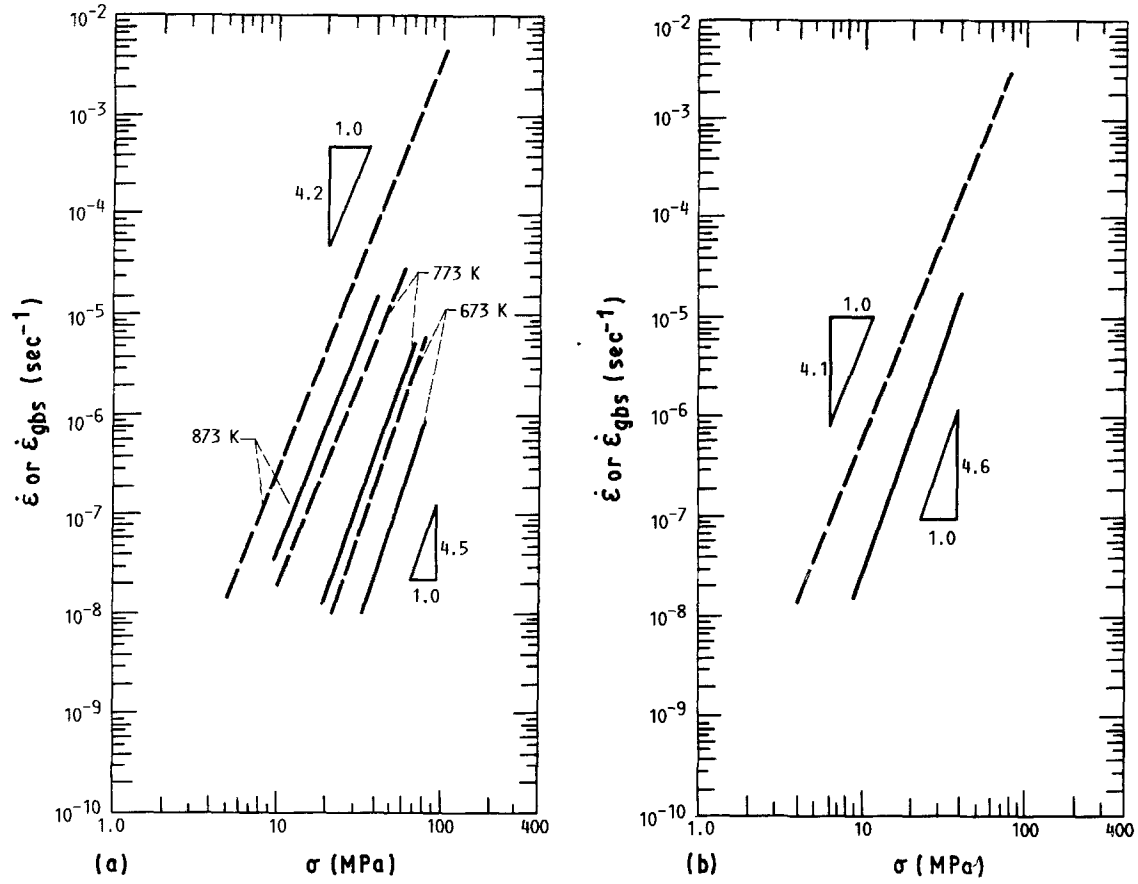

Figure 6 Variation of (———) the initial sliding strain rate, $\dot{\varepsilon}_{gbs}$, and (– – –) the steady-state creep rate, $\dot{\varepsilon}$, with stress for (a) copper, $d = 250$ μm and (b) Cu–30% Zn, $d = 120$ μm, $T = 823$ K, showing the similarities in the stress dependencies of both variables. The steady-state creep rate data on copper and Cu–30% Zn were obtained from [24] and [19], respectively.

135 kJ mol^{-1} at $\sigma/G = 2.0 \times 10^{-3}$ [23] under similar experimental conditions. Comparing the activation energies for creep and grain boundary sliding at similar values of σ/G at which these data were obtained, it is found that $0.77\ Q_c \leqslant Q_{gbs} \leqslant 1.55\ Q_c$ for polycrystalline copper. Similarly, noting that the activation energy for lattice diffusion, Q_l, in copper is about 210 kJ mol^{-1} [24], the magnitude of Q_{gbs} increases from about $0.57\ Q_l$ at the lower temperatures and higher stresses to about $1.33\ Q_l$ at the higher temperatures and lower stresses. In the case of Cu–30% Zn, Q_c exhibited a weaker dependence on the applied

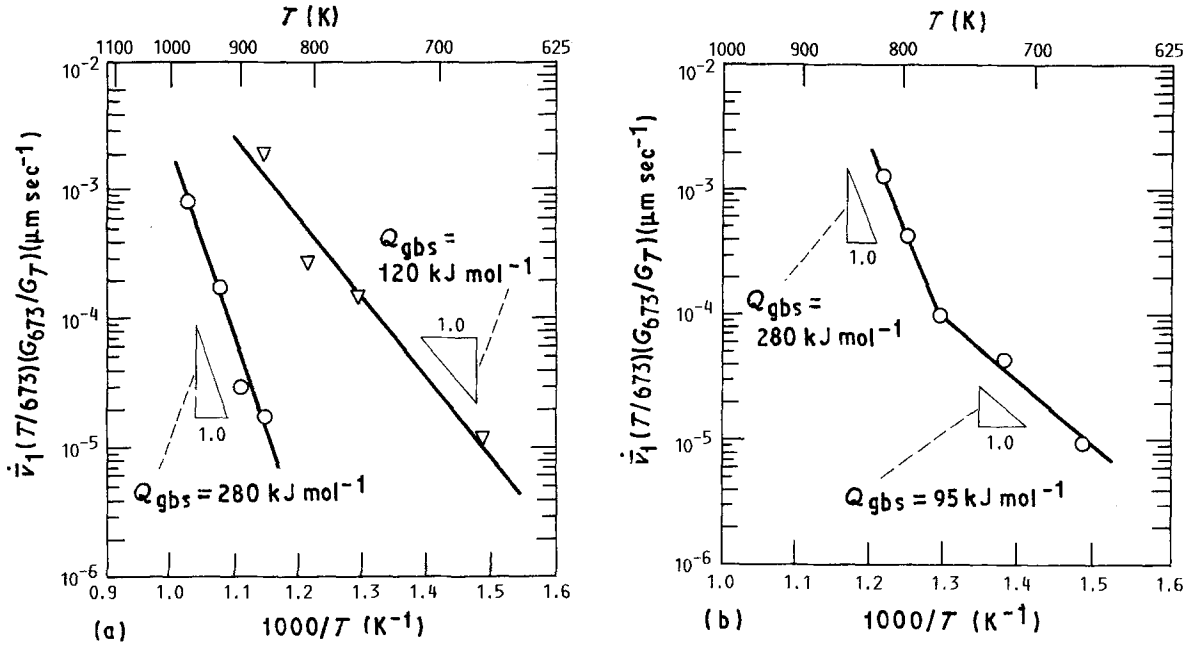

Figure 7 Plot of the temperature-compensated values of the mean sliding rate against the inverse of the absolute temperature for (a) copper, $d = 250$ μm and (b) Cu–30% Zn, $d = 120$ μm. The values of the shear modulus, G_T, at a particular temperature were obtained from [24] for copper and [19] for Cu–30% Zn. σ (MPa): (a) (○) 10.0, (▽) 39.8; (b) 39.7.

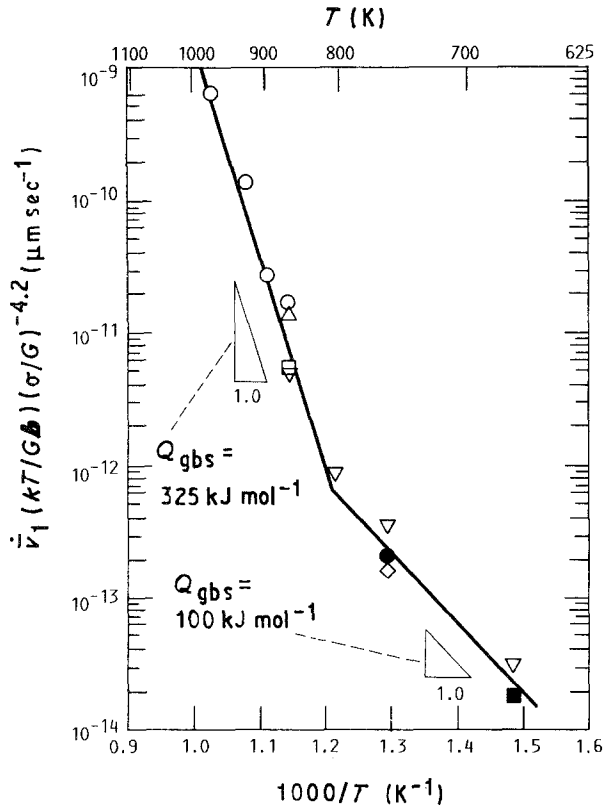

Figure 8 Plot of the stress and temperature-compensated values of the mean sliding rate against the inverse of the absolute temperature for copper, $d = 250$ μm. σ (MPa); (○) 10.0, (□) 15.8, (△) 24.1, (◇) 25.0, (▽) 39.8, (●) 62.1, (■) 79.0.

normalized stress with $Q_c \approx 180\,\text{kJ mol}^{-1}$ at $\sigma/G = 3.0 \times 10^{-4}$ and $Q_c \approx 170\,\text{kJ mol}^{-1}$ at $\sigma/G = 2.0 \times 10^{-3}$ [19]. Thus, $0.56\ Q_c \leqslant Q_{gbs} \leqslant 1.56\ Q_c$ for the data shown in Fig. 7b. Because the effective activation energy for diffusion in the alloy is about 180 kJ mol^{-1} [19], the magnitude of Q_{gbs} varies from about $0.53\ Q_l$ at the lower temperatures to about $1.56\ Q_l$ at the higher temperatures.

3. Discussion

It is clear from the review of experimental data presented in Section 2 that the characteristics of the grain boundary sliding mechanisms in copper and Cu–30% Zn are essentially similar, except for the fact that grain boundary sliding in the alloy is generally associated with an incubation period whenever the primary creep curve exhibits inverse, linear or sigmoidal behaviour. These results clearly demonstrate the influence of intragranular creep on grain boundary sliding. In addition, the observations of slide hardening in copper, an incubation period in the alpha brass, and the high values of Q_{gbs} suggest that sliding does not occur easily in these materials.

3.1. A compilation of activation energies for sliding in copper and Cu–30% Zn

The high values of $Q_{gbs} \gg Q_l$ (or Q_c) for copper and Cu–30% Zn do not agree with observations on other materials for which, in general, $0.6\ Q_l \leqslant Q_{gbs} \approx Q_l$ [25]. Fig. 9 shows the range of values of Q_{gbs} as a function of the absolute temperature reported in several investigations on copper bicrystals [21, 27, 28], and polycrystalline copper [18, 19] and alpha brass [19, 29]. The activation energies for lattice and intrinsic diffusion in copper and Cu–30% Zn, respectively, as well as the absolute melting temperatures for each material, are also indicated in the figure. The activation energies for intrinsic diffusion of copper and zinc in Cu–30% Zn, which were determined from a compilation of experimental diffusion data, were found to be $Q_{Cu} \approx 175\,\text{kJ mol}^{-1}$ and $Q_{Zn} \approx 165\,\text{kJ mol}^{-1}$, respectively [19].

A comparison of the bicrystal sliding data on copper indicates that the values of Q_{gbs} reported by Lagarde and Biscondi [28] are in good agreement with the observations of Watanabe and Davies [21] in a similar range of temperatures. However, both these sets of data have values of Q_{gbs} which are considerably less than those reported by Intrater and Machlin [27]. Considering the data for the polycrystalline materials shown in Fig. 9, it is seen that there is a tendency for the magnitude of Q_{gbs} to increase with grain size at the lower temperatures. There is also an apparent increase in the transition temperature at which $Q_{gbs} \gg Q_l$ with increasing grain size as is evident through a comparison of the data for copper and Cu–30% Zn [19]. It is obvious from Fig. 9 that there is a wide variation in the reported values of Q_{gbs} and in the nature of its temperature dependence for bicrystalline and polycrystalline copper. For example, for the bicrystal data reported by Lagarde and Biscondi [28], Q_{gbs} decreases from a value of about Q_l when $T < 720$ K to about $0.15\ Q_l$ when $T > 720$ K. In contrast, Q_{gbs} for polycrystalline copper [19] increases from about $0.57\ Q_l$ when $T < 873$ K to about $1.33\ Q_l$ for $T > 873$ K. This variation in the activation energies may be due to differences in the nature of the grain boundary sliding mechanism in bicrystals and polycrystals because sliding in the latter must be accommodated at the triple points [25]; in contrast, there are no triple points to hinder sliding in bicrystals.

3.2. Evaluation of grain boundary sliding models

Grain boundary sliding mechanisms fall into two categories: intrinsic and extrinsic models, and these are discussed in detail by Langdon and Vastava [25]. As shown in Table I, the intrinsic sliding models [14, 21, 30, 31] typically predict a value of $n_{gbs} = 1$ and $Q_{gbs} = Q_{gb}$, where Q_{gb} is the activation energy for grain boundary diffusion. Because $n_{gbs} \approx 4.2$ to 4.6 for copper and Cu–30% Zn (Section 2.3), it can be concluded that the intrinsic grain boundary sliding mechanisms are not important in these polycrystalline materials. Similarly, Langdon and Vastava [25] have demonstrated that the experimental value of n_{gbs} are greater than 1.0 for other polycrystalline materials.

A number of mechanisms have been proposed for polycrystalline materials which differ from each other based on the nature of the accommodating process [25]. The values of n_{gbs} and Q_{gbs} predicted by these

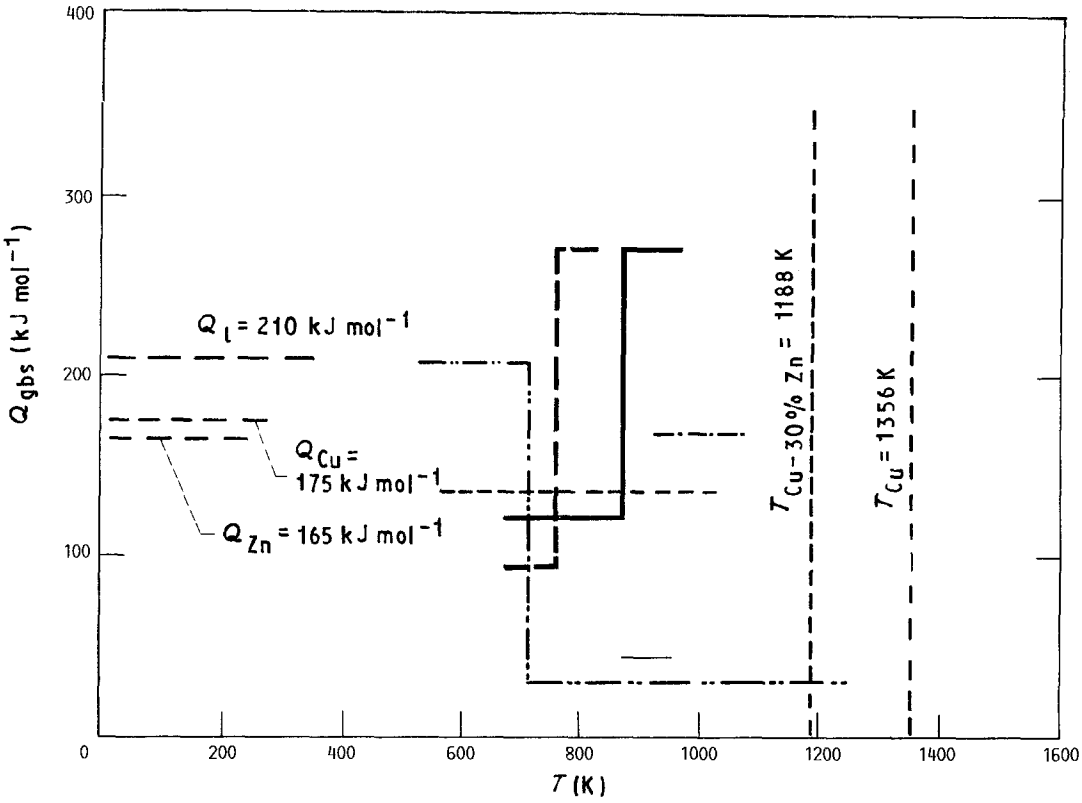

Figure 9 Variation of Q_{gbs} with the absolute temperature for copper bicrystals [21, 27, 28], and polycrystalline copper [19] and Cu–30% Zn [19, 29]. The values of $Q_l \approx 210$ kJ mol^{-1} for copper [24], and $Q_{Cu} \approx 175$ kJ mol^{-1} and $Q_{Zn} \approx 165$ kJ mol^{-1} for Cu–30% Zn [19] are also indicated in the figure. (—·—) copper bicrystals [27], (—··—) copper bicrystals [28], (———) copper bicrystals [21], (———) copper, $d = 250$ μm [19], (– – –) alpha brass, $d = 470$ μm [29], (— — —) alpha brass, $d = 120$ μm [19].

models are compared in Table II with the experimental data on polycrystalline copper and alpha brass discussed in Section 2.0, where Q_{gbm} is the activation energy for grain boundary migration. Assuming that Q_{gbm} and Q_{gb} are equal to about 0.5 Q_l, it is evident from Table II that the predicted magnitudes of Q_{gbs} do not agree with the experimental data obtained on copper and Cu–30% Zn when $T > 873$ and 770 K, respectively. In addition, the values of n_{gbs} predicted by the Langdon [32], Gifkins [33], and the Crossman and Ashby [34] models do not agree with the experimental values at all temperatures. Although the magnitudes of n_{gbs} and Q_{gbs} predicted by the Nix model

TABLE I Values of n_{gbs} and Q_{gbs} for intrinsic grain boundary sliding models

Model	n_{gbs}	Q_{gbs}	Mechanism
Raj and Ashby [14]	1.0	Q_{gb}	Diffusional accommodation
Watanabe and Davies [21]	1.0	–	Glide and climb of components of a lattice dislocation in the grain boundary
Gates [30]	1.0	Q_{gb}	Glide and climb of grain boundary dislocations
Ponds *et al.* [31]	1.0	Q_{gb}	Dislocation climb in the grain boundary plane

TABLE II Comparison of (a) grain boundary sliding models for polycrystalline materials with (b) the experimental results on copper and alpha brass

(a) Grain boundary sliding models

Model	n_{gbs}	Q_{gbs}	Mechanism
Nix [18]	4.0	Q_{gbm}	Grain boundary migration coupled with sliding
Langdon [32]	2.0	Q_l	Dislocation climb and glide near grain boundaries
Gifkins [25, 33]	3.5	Q_l	Triple-point fold formation
Crossman and Ashby [34]	1.0	Q_{gb}	Intragranular power-law creep

(b) Experimental results on copper and alpha brass [19]

Material	T (K)	σ (MPa)	n_{gbs}	Q_{gbs}/Q_l
Cu	673–873	39.8	4.2–4.5	0.6[a]
	873–973	10.0	4.5	1.3[a]
Cu–30% Zn	673–770	39.7	–	0.5[b]
	770–823	39.7	4.6	1.6[b]

[a] $Q_l = 210$ kJ mol^{-1} [24]. Grain boundary migration was observed at a few isolated boundaries only when $T \geqslant 873$ K.
[b] $Q_l = 180$ kJ mol^{-1} [19]. This value was estimated from equations for complex diffusivity for viscous glide and climb-controlled intragranular mechanisms [35–37] using tracer diffusion data for copper and zinc in the alloy [19]. An identical value of Q_l was obtained for both types of intragranular creep mechanisms.

[18] are in reasonable agreement with the experimental data below the transition temperature, this agreement must be considered fortuitous because no grain boundary migration was observed at these temperatures and stresses. It is therefore concluded that the current models for grain boundary sliding do not adequately describe the sliding behaviour in polycrystalline copper and alpha brass. This discrepancy between theory and experiment has also been reported for other materials [25].

3.3. A phenomenological model for sliding

The observation of an incubation period for sliding in Cu–30% Zn is significant. The close correspondence between the occurrence of sigmoidal or inverse primary creep and an incubation period for sliding suggests that the grain boundary sliding mechanism is influenced by the mobile dislocation density in the grain interior, because it is now generally accepted that sigmoidal and inverse primary creep in solid solution alloys result from a low initial mobile dislocation density [38]. Therefore, it follows that no incubation period would be observed when a sufficient number of mobile dislocations are active in the grain interior during creep, as would be the case when a normal primary transient is observed. The observations on copper (Fig. 2) and Cu–30% Zn (Fig. 3) are consistent with this viewpoint. This rationale suggests that the grain boundary sliding behaviour in both materials is influenced by intragranular creep which is consistent with other observations reported in Section 2.

More importantly, the values of $Q_{gbs} \gg Q_l$, and its dependence on stress and temperature, suggest that the rate-controlling mechanism for grain boundary sliding at intermediate temperatures is non-diffusional in nature. Therefore, any mechanism proposed to explain these results on copper and alpha brass must consider this fact, together with the role of lattice deformation on sliding. A probable mechanism for grain boundary sliding is shown in Fig. 10, where it is assumed that slip on the primary glide plane leads to a build-up of stress at its intersection with the grain boundary at C (Fig. 10a) and the formation of a ledge (Fig. 10b). In the absence of diffusional relaxation of this stress concentration, slip can commence on a secondary slip plane close to the grain boundary when the resolved magnitude of this stress concentration exceeds the critical resolved shear stress, τ_s, for that plane thereby resulting in sliding at the boundary (Fig. 10b). Thus, the rate of glide of the secondary dislocations would govern the rate of sliding.

By its very nature, the model predicts that the amount of sliding would vary along the boundary, and these localized variations in the extent of sliding were observed quite frequently [19]. Furthermore, the model suggests that sliding can become difficult under certain circumstances such as: a decrease in the number of primary dislocations; the unavailability of sufficient number of secondary slip systems; a relaxation of the stress concentration at C in Fig. 10a due to recovery; or a decrease in the stress concentration due

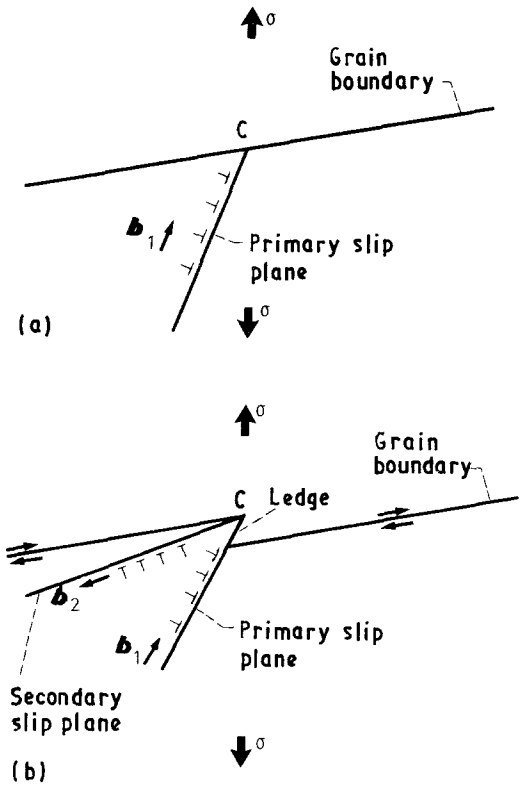

Figure 10 Phenomenological model for grain boundary sliding. (a) Primary slip leads to a build-up of stress at C, and a ledge as shown in (b). Secondary slip occurs in the absence of a relaxation of this stress concentration which results in grain boundary sliding.

to cavitation. These factors can individually or collectively result in high values of Q_{gbs}, a tendency towards slide hardening, and the observation of an incubation period for sliding. For example, recent observations of surface slip features on copper showed relatively few primary slip lines under conditions when $Q_{gbs} \gg Q_c$, whereas cross slip and secondary slip features were observed extensively when $Q_{gbs} < Q_l$ [19]. Similarly, as discussed in Section 2.1, the observation of an incubation period for sliding in alpha brass appears to be related to a low initial mobile dislocation density.

4. Conclusions

1. An examination of grain boundary sliding data obtained on copper and Cu–30% Zn showed that ξ varies between 40% and 50% during the initial stages of creep but it decreases rapidly with increasing strain to less than 10% when $\varepsilon > 5\%$.

2. The grain boundary sliding behaviour in these materials is influenced by the deformation processes occurring within the grain interior as indicated by the observation of an incubation period for sliding in the alloy, the strong correlation between ξ and ε, and the similarities in the values of $n \approx n_{gbs} \approx 4.5$.

3. The activation energy for grain boundary sliding in copper and Cu–30% Zn varies between about $0.50\,Q_c$ and $1.60\,Q_c$, and it increases with decreasing stress and increasing temperature.

4. Several models for grain boundary sliding are reviewed briefly and it is shown that they are not consistent with the experimental observations.

5. A phenomenological model is proposed which assumes that primary slip leads to a stress concentration at the intersection of the primary glide plane and the grain boundary. It is suggested that sliding results when the magnitude of this stress concentration exceeds the critical resolved shear stress of a secondary slip system close to the grain boundary.

Acknowledgements

This investigation was supported by a grant from the NASA Lewis Research Center. The experimental data reported in this paper were obtained at the University of Southern California, Los Angeles under a programme funded by the United States Department of Energy.

References

1. W. D. NIX and J. C. GIBELING, in "Flow and Fracture at Elevated Temperatures", edited by R. Raj (American Society for Metals, Metals Park, Ohio, 1985) p. 1.
2. A. W. MULLENDORE and N. J. GRANT, *Trans. AIME* **227** (1963) 319.
3. H. J. WESTWOOD and D. M. R. TAPLIN, *J. Mater. Sci.* **20** (1975) 141.
4. R. L. BELL and T. G. LANGDON, *ibid.* **2** (1967) 313.
5. R. L. BELL and T. G. LANGDON, in "Interfaces Conference", edited by R. C. Gifkins (Butterworths, Sydney, 1969) p. 115.
6. H. GLEITER and B. CHALMERS, *Prog. Mater. Sci.* **16** (1972) 179.
7. V. SKLENIČKA, K. PROCHÁZKA and J. ČADEK, *Z. Metallkde* **63** (1973) 65.
8. T. G. LANGDON, in "Deformation of Ceramic Materials", edited by R. C. Bradt and R. E. Tressler (Plenum Press, New York, 1975) p. 101.
9. R. C. GIFKINS, *Metall. Trans.* **8A** (1977) 1507.
10. R. S. GATES, *Mater. Sci. Engng* **27** (1977) 115.
11. T. G. LANGDON, in "The Microstructure and Design of Alloys: Proceedings of the Third International Conference on the Strength of Metals and Alloys", Vol. 1 (The Institute of Metals and The Iron and Steel Institute, London, 1973) p. 222.
12. R. S. GATES and C. A. P. HORTON, *Mater. Sci. Engng* **27** (1977) 105.
13. W. R. CANNON, *Phil. Mag.* **25** (1972) 1489.
14. R. RAJ and M. F. ASHBY, *Metall. Trans.* **2** (1971) 1113.
15. F. R. N. NABARRO, in "Report of a Conference on Strength of Solids" (The Physical Society, London, 1948) p. 75.
16. C. HERRING, *J. Appl. Phys.* **21** (1950) 437.
17. R. L. COBLE, *ibid.* **34** (1963) 1679.
18. W. D. NIX, in "Rate Processes in Plastic Deformation of Materials", edited by J. C. M. Li and A. K. Mukherjee (American Society for Metals, Metals Park, Ohio, 1975) p. 384.
19. S. V. RAJ, PhD thesis, University of Southern California, Los Angeles (1984).
20. T. G. LANGDON, *Metals Forum* **4** (1981) 14.
21. T. WATANABE and P. W. DAVIES, *Phil. Mag.* **37** (1978) 649.
22. R. L. BELL, N. B. W. THOMPSON and P. A. TURNER, *J. Mater. Sci.* **3** (1968) 524.
23. T. WATANABE, M. YAMADA, S. SHIMA and S. KARASHIMA, *Phil. Mag.* **40** (1979) 667.
24. S. V. RAJ and T. G. LANGDON, *Acta Metall.* **37** (1989) 843.
25. T. G. LANGDON and R. B. VASTAVA, in "Mechanical Testing for Deformation Model Development, ASTM (STP) 765", edited by R. W. Rhode and J. C. Swearengen (American Society for Testing and Materials, Philadelphia, Pennsylvania, 1982) p. 435.
26. R. C. GIFKINS, in "Creep and Fracture of Engineering Materials and Structures", edited by B. Wilshire and R. W. Evans (The Institute of Metals, London, 1987) p. 141.
27. J. INTRATER and E. S. MACHLIN, *J. Inst. Metals* **88** (1959–60) 305.
28. P. LAGARDE and M. BISCONDI, *Mem. Sci. Rev. Metall.* **71** (1974) 121.
29. V. SKLENIČKA, I. SAXL, J. POPULE and J. ČADEK, *Mater. Sci. Engng* **18** (1975) 271.
30. R. S. GATES, *Acta Metall.* **21** (1973) 855.
31. R. C. POND, D. A. SMITH and P. W. J. SOUTHERDEN, in "Proceedings of the 4th International Conference on the Strength of Metals and Alloys", Vol. 1 (Laboratoire de Physique du Solide, E. N. S. M. I. M., Nancy, France, 1976) p. 378.
32. T. G. LANGDON, *Phil. Mag.* **22** (1970) 689.
33. R. C. GIFKINS, *J. Austral. Inst. Metals* **18** (1973) 137.
34. F. W. CROSSMAN and M. F. ASHBY, *Acta Metall.* **23** (1975) 425.
35. R. FUENTES-SAMANIEGO, W. D. NIX and G. M. POUND, *Phil. Mag.* **42A** (1980) 591.
36. R. FUENTES-SAMANIEGO and W. D. NIX, *Scripta Metall.* **15** (1981) 15.
37. R. FUENTES-SAMANIEGO, W. D. NIX and G. M. POUND, *Acta Metall.* **29** (1981) 487.
38. W. D. NIX and B. ILSCHNER, in 'Strength of Metals and Alloys (ICSMA 5)", Vol. 3, edited by P. Haasen, V. Gerold and G. Kostorz (Pergamon Press, Oxford, 1980) p. 1503.

Received 15 May
and accepted 23 October 1989